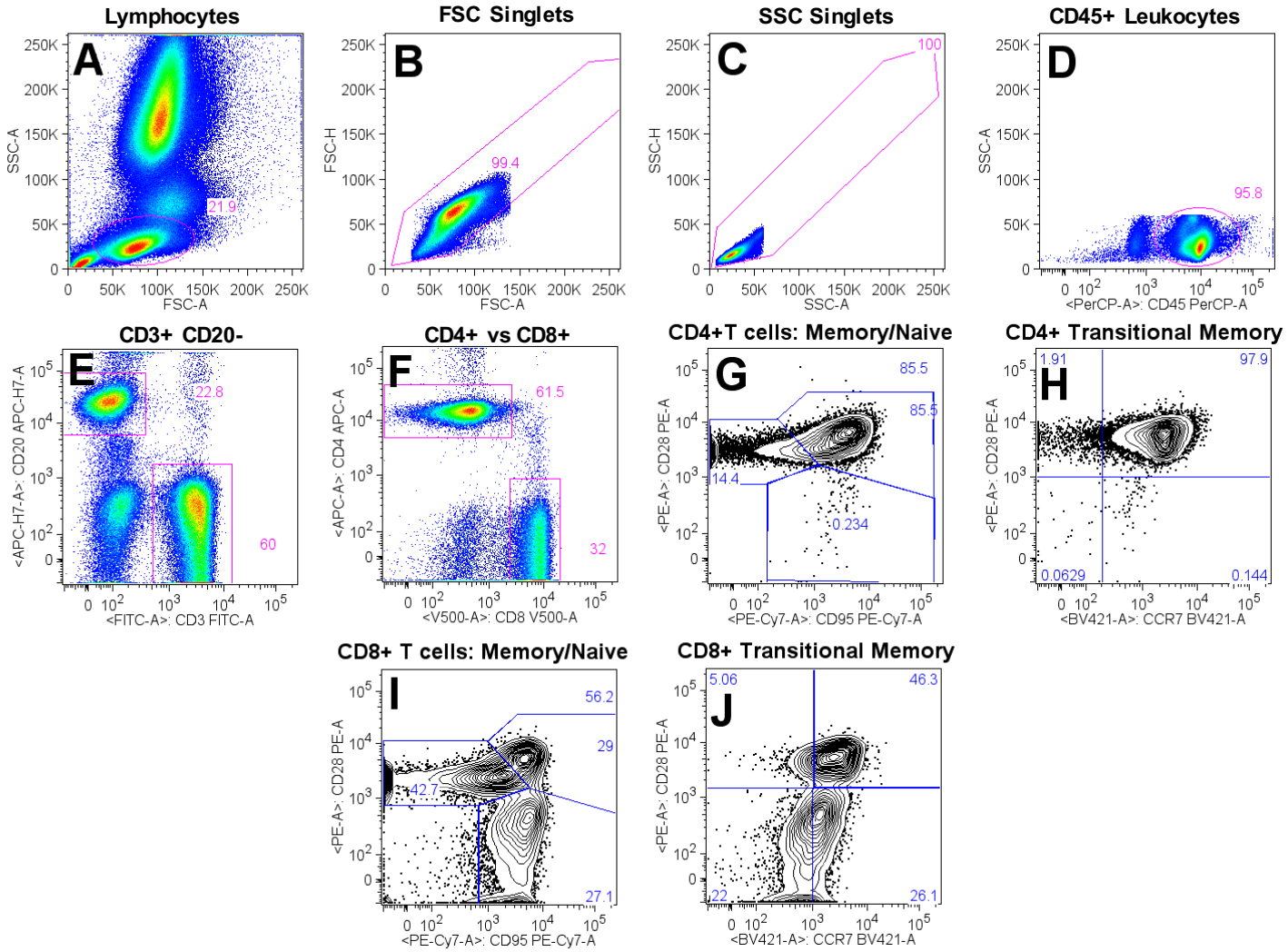

Supplemental Figure 1. Flow cytometry gating of peripheral blood mononuclear cells for T cell phenotyping. A generous lymphocyte gate was applied (**A**), then FSC singlets (**B**), SSC singlets (**C**), and CD45+ leukocytes (**D**) were selected. Next, the CD3+ T cell population was identified (**E**), and CD4+ and CD8+ T cell populations defined **(F).** Central memory , effector memory, and naïve CD4+ and CD8+ T cell subsets were classified as either CD28+CD95+, CD28- CD95+, and CD28+CD95-, respectively (**G,I**). Transitional memory T cells were characterized as CD28+CCR7- (**H,J**).

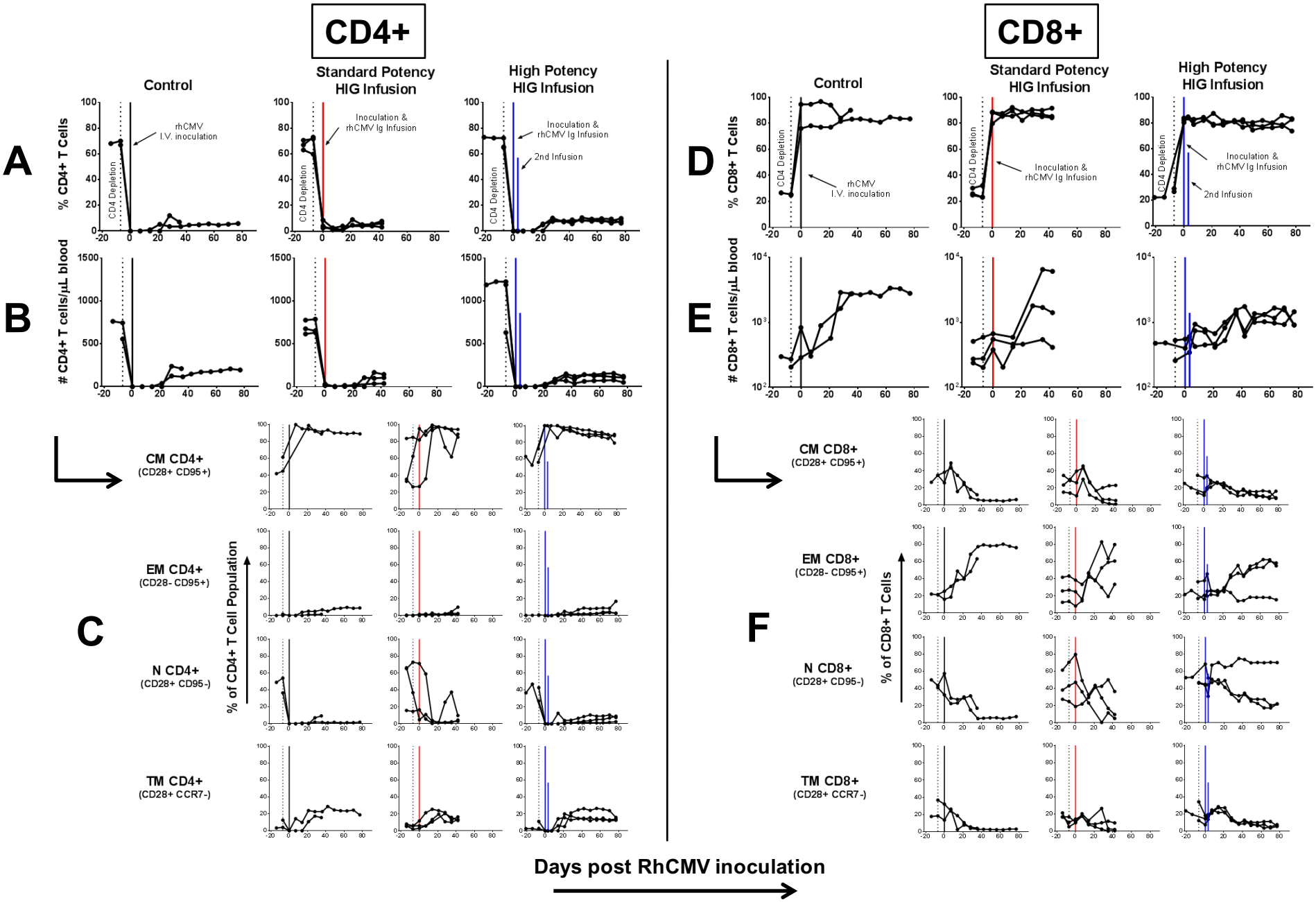

Supplemental Figure 2. Peripheral CD4+ and CD8+ T cell kinetics and subset proportions are similar between treatment groups following CD4+ T cell depletion by anti-CD4+ mAb infusion. Legend next page.

Supplemental Figure 2. Peripheral CD4+ and CD8+ T cell kinetics and subset proportions are similar between treatment groups following CD4+ T cell depletion by anti-CD4+ mAb infusion. Both the percentage of peripheral CD4+ T cells (**A**) and the absolute number of peripheral CD4+ T cells (**B**) declined dramatically in all animals following administration of CD4+ T cell depleting antibody (CD4R1 clone), as indicated by vertical dotted black line, and remained suppressed without full recovery throughout the study. The percentages of central memory (CM) CD4+ T cells (CD28+CD95+), effector memory (EM) CD4+ T cells (CD28-CD95+), naïve (N) CD4+ T cells (CD28+CD95-), and transitional memory (TM) CD4+ T cells (CD28+CCR7-) are similar between treatment groups (**C**), with CM cells representing the dominant phenotype in the recovering population. Following CD4+ T cell depletion and RhCMV infection, both the relative percentage of peripheral CD8+ T cells (**D**) and the absolute number of peripheral CD8+ T cells (**E**) increased in all animals. Furthermore, analysis of CD8+ T cell subsets including central memory (CM) CD8+ T cells (CD28+CD95+), effector memory (EM) CD8+ T cells (CD28-CD95+), naïve (N) CD8+ T cells (CD28+CD95-), and transitional memory (TM) CD8+ T cells (CD28+CCR7-) (**F**) demonstrated that the EM population generally increased over time and CM/N/TM populations declined in a pattern consistent with primary infection.

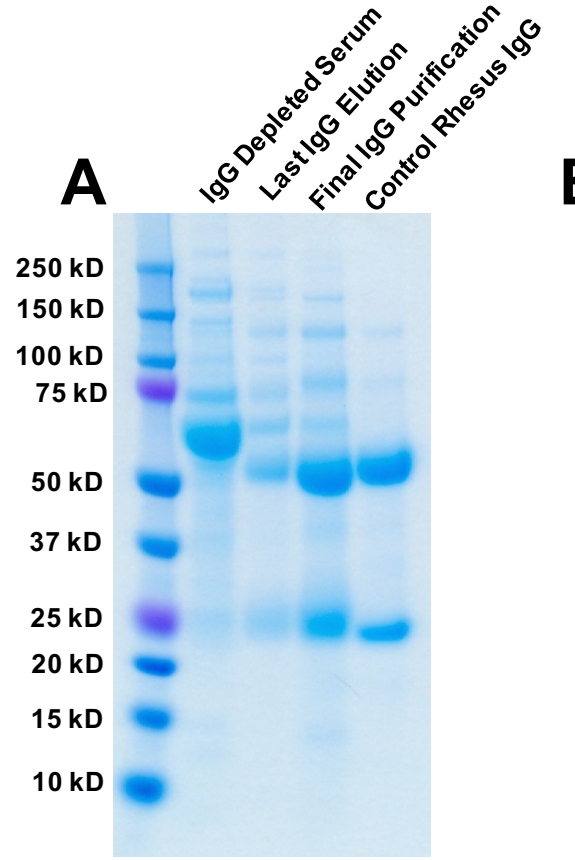

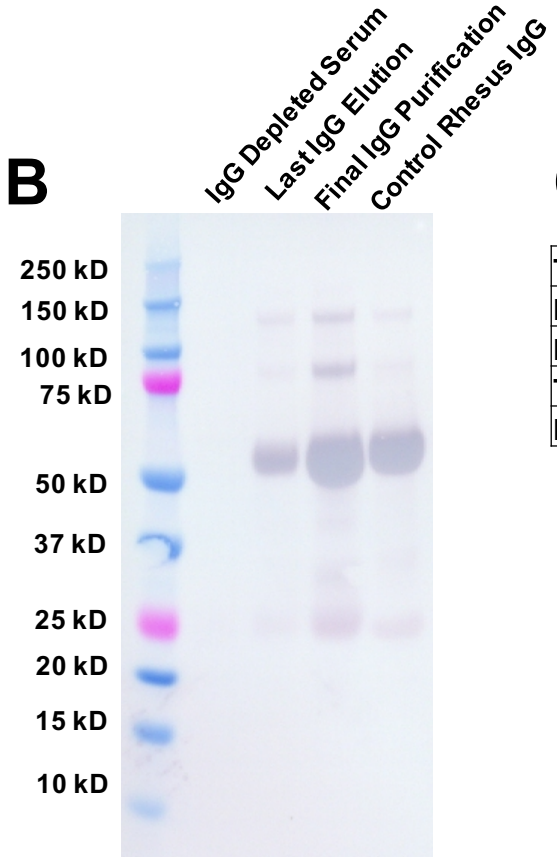

C

Total Rhesus Plasma	907 ml
Final IgG Conc.	106.9 mg/ml
Final IgG Volume	55 ml
Total Rhesus IgG	5879.5 mg
Endotoxin	0.0189 EU/ml

Supplemental Figure 3. Quality control of purified high-potency RhCMV HIG product. (**A**) Coomassie under reducing conditions showing high-potency HIG preparation purified from RhCMV-seropositive rhesus plasma (3rd column). (**B**) Western blot under reducing conditions demonstrating high-potency HIG preparation detected by rabbit anti-monkey IgG-AP showing absence of IgG in depleted sera (1st column) as well as distinct heavy and light chain bands (3rd column – 55 and 25kDa) (**C**) Details regarding the purification process and final composition and endotoxin levels of the high-potency HIG product.

A **PK modeling parameters for two-compartment model**

Body weight normalized PK parameters	Standard Potency HIG Infused		Dose-optimized, high-potency HIG infused	
	Mean (n=3)	SD (n=3)	Mean (n=3)	SD (n=3)
Volume 1 (mL/kg)	42.9	14.9	42.1	11.9
Clearance (mL/day/kg)	6.43	1.06	6.34	1.59
Volume 2 (mL/kg)	26.0	10.3	19.3	8.82
Distribution Clearance (mL/day/kg)	7.13	5.66	71.3	102
Half-life (day)	4.54	0.825	7.13	0.329

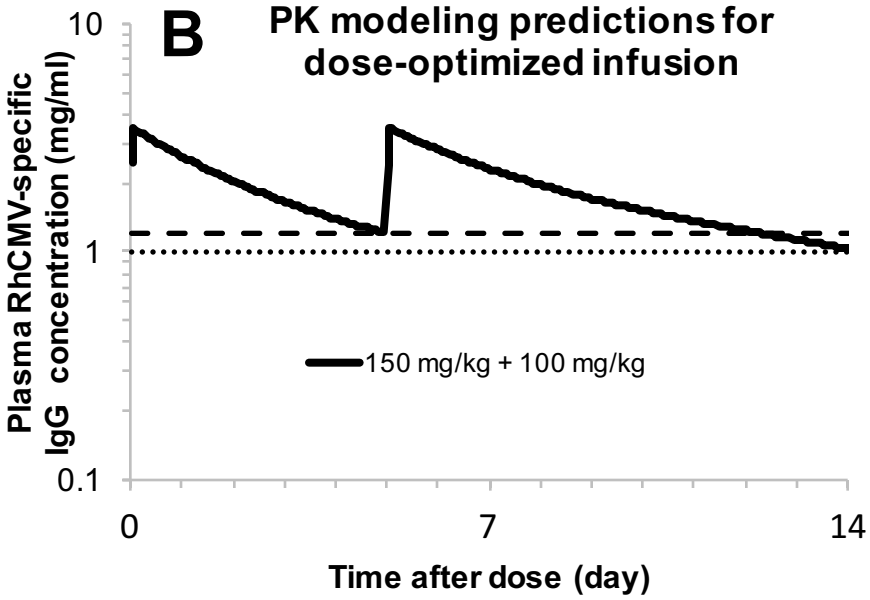

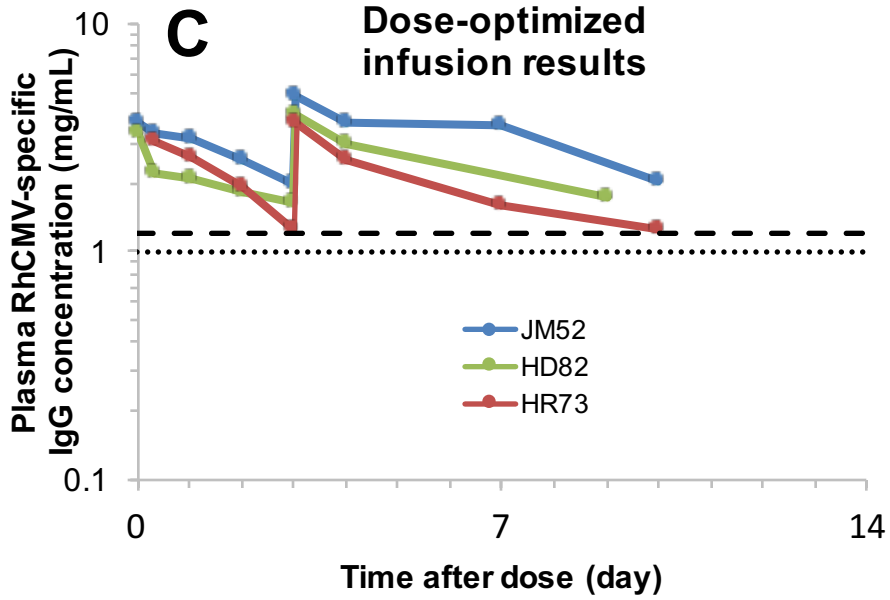

Supplemental Figure 4. Pharmacokinetic (PK) modeling for dose-optimization of high-potency HIG infusion. (**a**) PK coefficients were calculated using a two-compartment model system for standard HIG infusion and dose-optimized, high-potency HIG infusion. (**b**) An initial loading dose of 150mg/kg followed by a second dose of 100mg/kg 3 days later was determined to be the optimal regimen to maintain a level of infused IgG above 1-1.2mg/mL (estimated epithelial ID_{50} of 1000; horizontal dotted black lines), for 14 days. (**c**) HIG infusion kinetics for high potency HIG infused animals accurately mimicked the PK prediction.

A

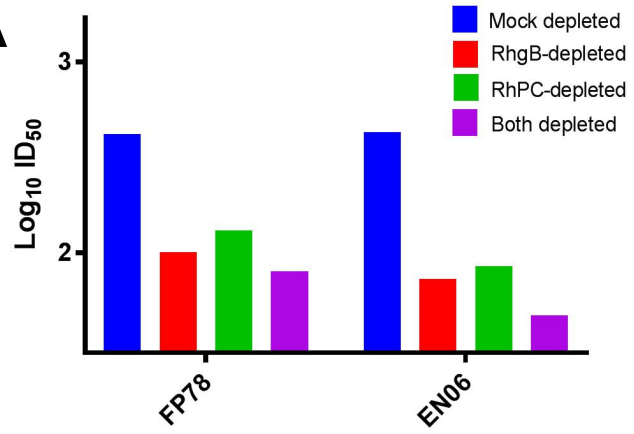

B

	FP78			EN06		
	RhgB ED_{50}	RhPC ED_{50}	**ID_{50}**	RhgB ED_{50}	RhPC ED_{50}	**ID_{50}**
Mock depleted	537	370	**420**	2184	86	**430**
RhgB-depleted	<30	357	**101**	<30	112	**73**
RhPC-depleted	312	79	**131**	1190	<30	**85**
Both depleted	<30	51	**80**	122	<30	**47**

Supplemental Figure 5. Both RhCMV gB and PC-specific antibodies contribute to neutralization activity of individual RhCMV-seropositive rhesus monkeys. (**A**) ID_{50} values depict the relative neutralization potency of mock-depleted, RhgB-depleted, PC-depleted, and both RhgB/RhPC-depleted antibody preparations. (**B**) ID_{50} values for depleted antibodies measured in epithelial cells with UCD52 virus (starting dilution 1:10). ELISA ED_{50} values confirm specific depletion of antibodies for a given antigen (starting dilution 1:30). Each data point represents the mean value of two experimental replicates.

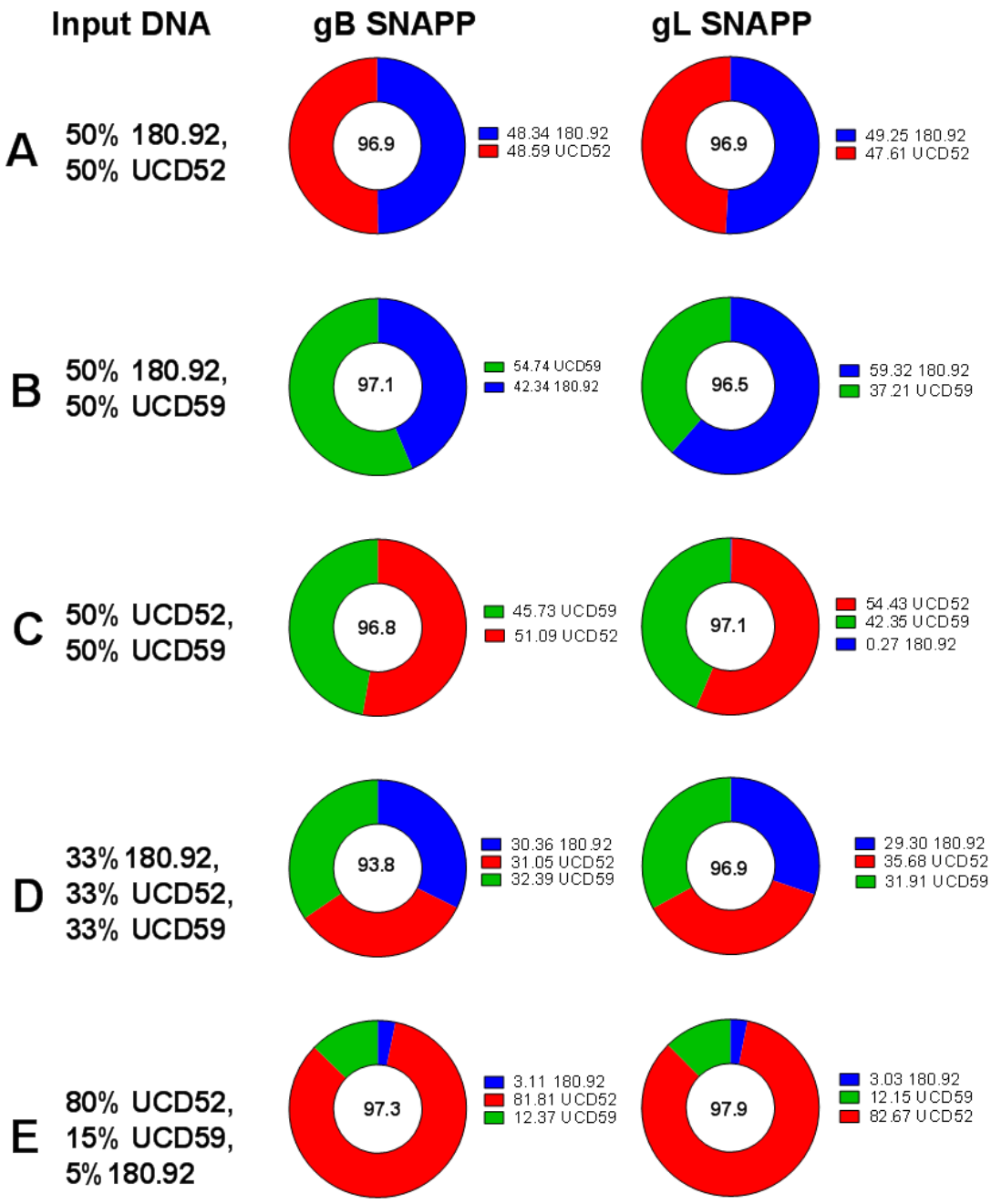

Supplemental Figure 6. Short NGS Amplicon Population Profiling (SNAPP) accurately reflects input strain-specific viral DNA. (**A**) Viral DNA from RhCMV viral strains 180.92 and UCD52 mixed in equal proportions (50% 180.92 + 50% UCD52), then sequenced by SNAPP at the gB and gL loci results in raw sequencing reads of 180.92 and UCD52 corresponding to the original ratio of input DNA. This result is replicated for RhCMV viral DNA mixed in various ratios (**B-E**). The number in center of each ring represents percentage of sequenced reads passing quality filters. The percentage of input reads corresponding to individual viral strains is denoted by the legend adjacent to each plot.

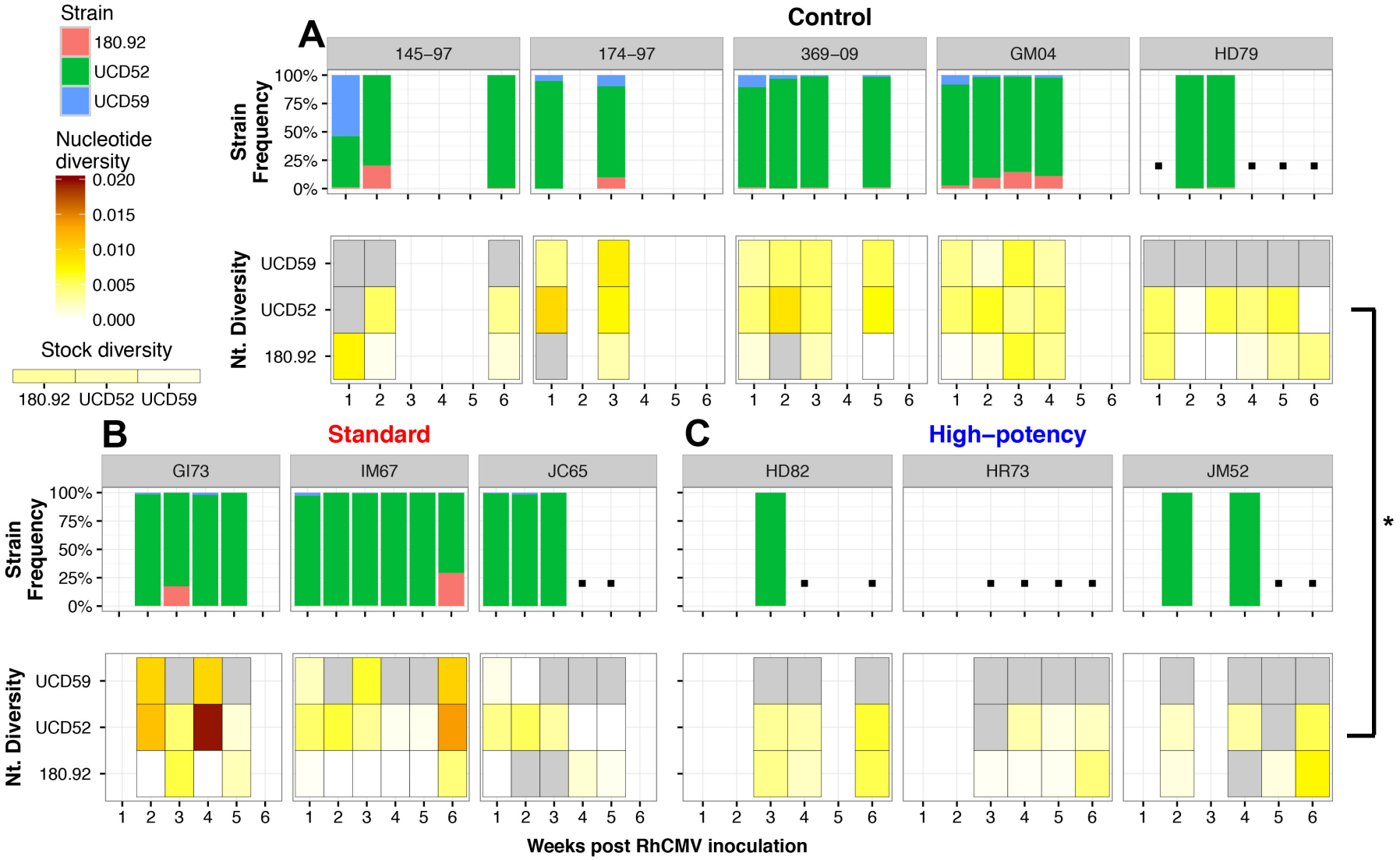

Supplemental Figure 7. Glycoprotein L SNAPP confirms restricted plasma viral diversity in high-potency HIG group.

Legend next page

Supplemental Figure 7. Glycoprotein L SNAPP confirms restricted plasma viral diversity in high-potency HIG group. Analogous to Fig 4, deep-sequencing analysis for maternal plasma virus population is shown for (**A**) 5 control dams (145-97, 174,97, 369-09, GM04, and HD79), (**B**) 3 standard HIG infused dams (GI73, IM67, and JC65), and (**C**) 3 high-potency HIG infused dams (HD82, HR73, and JM52). The **upper panel** indicates the percentage of sequence reads corresponding to each of the three inoculated RhCMV strains in plasma at weeks 1-6 post infection (180.92 in pink, UCD52 in green, and UCD59 in blue), which was similar between the treatment groups. ■ denotes samples amplified by nested PCR with known primer bias. The **lower panel** for each animal is a heat map depiction of viral nucleotide diversity (π), calculated as the mean π value across each sample's haplotype sequences. Scale ranges from white (π=0) to dark red (π=0.02). Gray coloring indicates that no sequence reads were detected at that time point for a given viral variant. Blank areas represent sample non-availability (control group) or limited plasma viral load (<100 copies/mL). There is a significant reduction in diversity at the gL locus for the dominant strain in plasma (UCD52) following high-potency HIG infusion (*p=0.036, Wilcoxon exact test). Each data point represents the mean value of two or more experimental replicates. Historical control animal 274-98 was omitted from this analysis because it was only inoculated with a single strain (180.92).

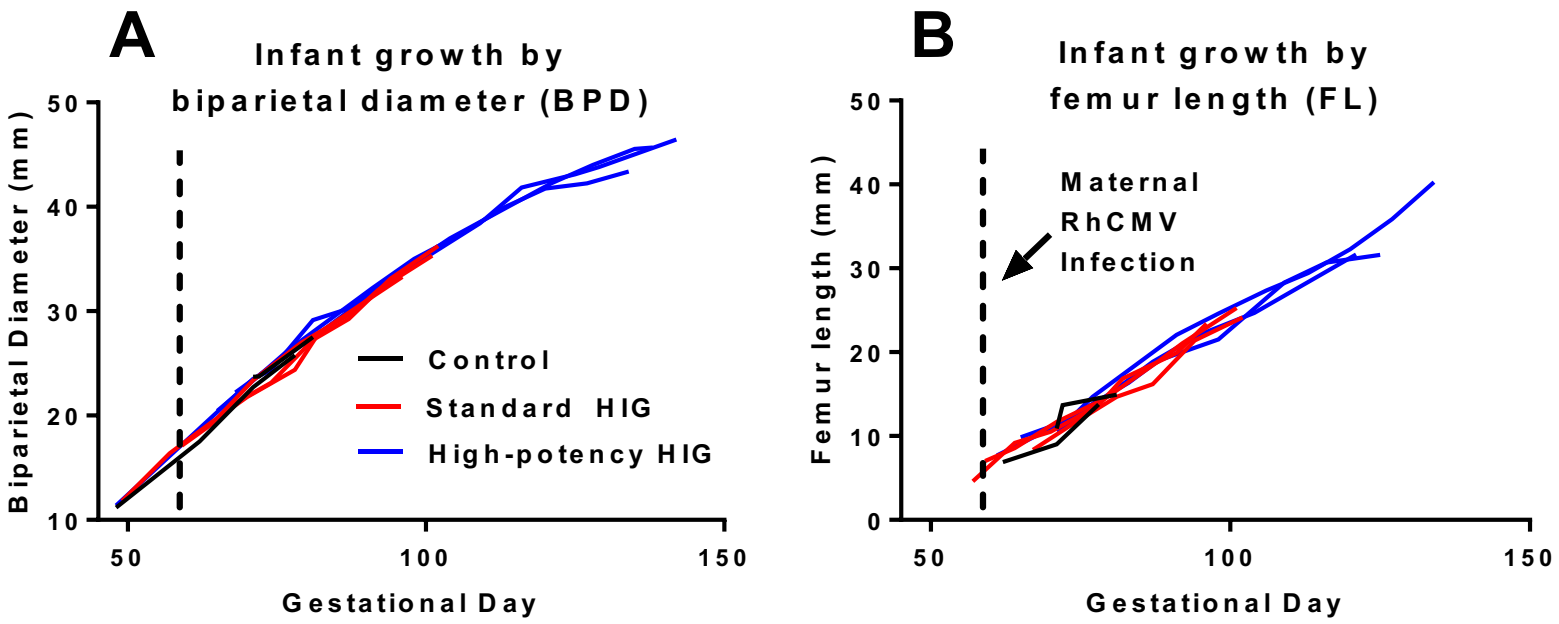

Supplemental Figure 8. Growth of RhCMV infected rhesus monkey fetuses is similar between control and HIG pretreatment groups. Fetuses were monitored regularly for signs of intrauterine growth restriction by ultrasound examination. Growth was measured by (**A**) biparietal diameter (BPD) and **(B)** femur length, and was within normal limits for all animals

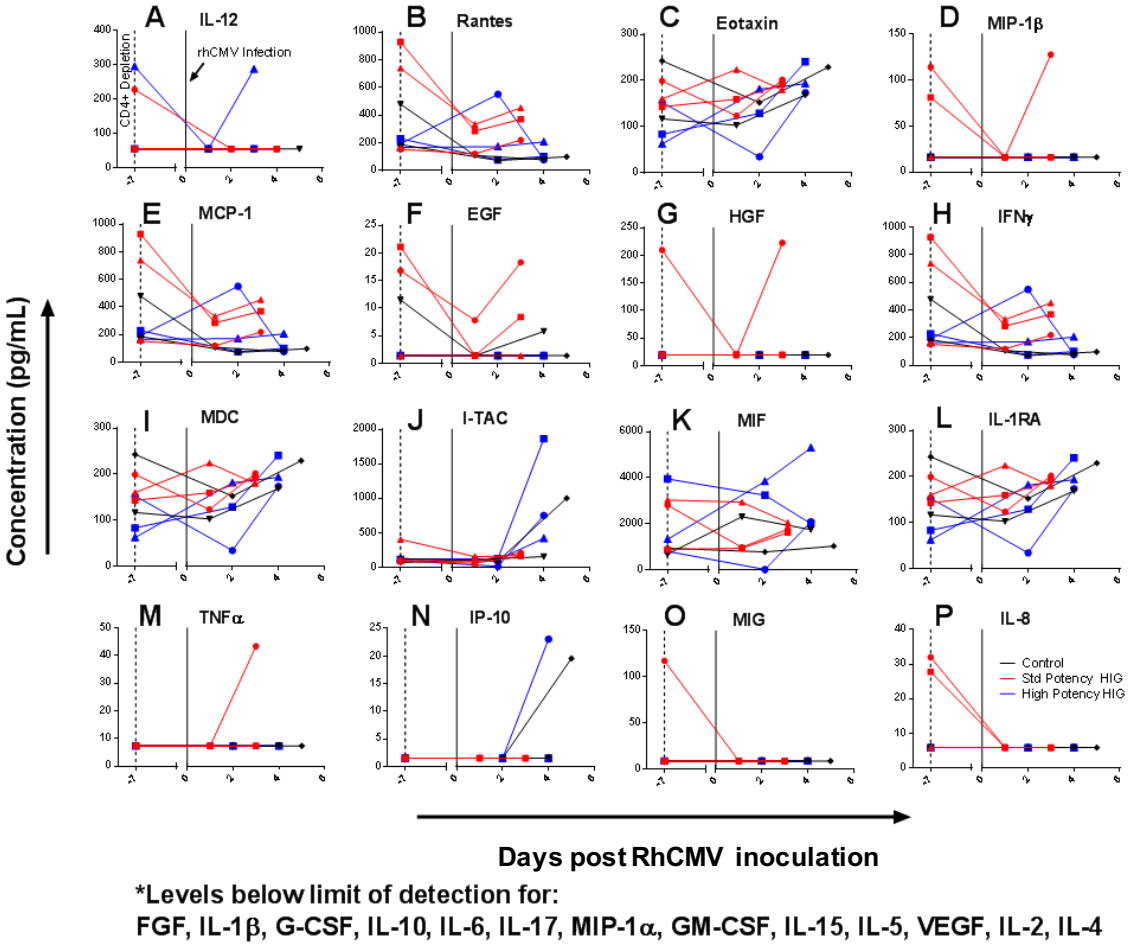

Supplemental Figure 9. Plasma cytokine and growth factor profile of RhCMV-infected rhesus dams is similar between control and HIG pre-treatment groups. 16 cytokines were detectable above background levels at one or more of the tested time points: IL-12 **(A),** Rantes (CCL5) (**B**), Eotaxin (**C**), MIP-1β (CCL4) (**D**), MCP-1 (**E**), EGF (**F**), HGF (**G**), IFNγ (**H**), MDC (CCL22) (**I**), I-TAC (CXCL11) (**J**), MIF (**K**), IL-1RA (**L**), TNFα (**M**), IP-10 (CXCL10) (**N**), MIG (CXCL9) (**O**), and IL-8 (**P**). Dotted vertical line indicates time of CD4+ T cell depletion, and solid vertical line indicates time of RhCMV infection. Two experimental replicates were completed for each data point.

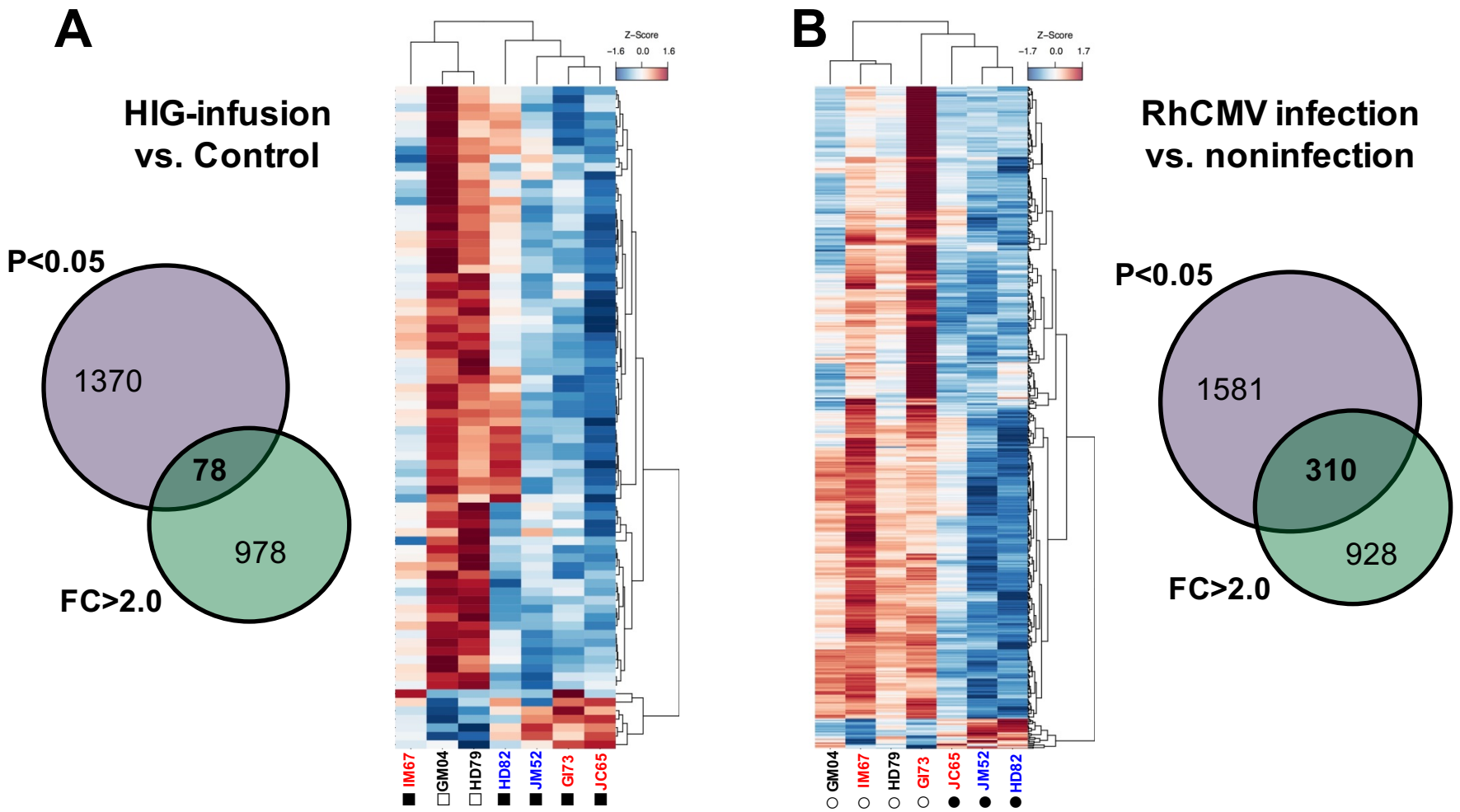

Supplemental Figure 10. Placental transcriptome is influenced more by RhCMV infection than HIG pretreatment or the outcome of fetal loss. (**A**) Heat map and Venn diagram for 78 differentially-expressed genes (p<0.05, fc>2.0) for dams with protected fetuses vs. dams with fetal loss (■=HIG pre-treatment/fetal survival; □=fetal loss) (**B**) Heat map and Venn diagram for 310 differentially-expressed genes (p<0.05, fc>2.0) for RhCMV-transmitting vs. nontransmitting dams (●=no RhCMV placental transmission; ○=placental transmission). Samples and genes are clustered based on correlation distance with complete linkage. A single transcriptome microarray was completed for each sample.

Marker	Fluorophore	Clone	Manufacturer	Staining
CCR7	FITC	150503	R&D Systems	Surface
CD95	PE	DX2	BD Biosciences	Surface
CD28	PerCP-Cy5.5	L293	BD Biosciences	Surface
CD4	PE-Cy7	L200	BD Biosciences	Surface
CD20	APC	L27	BD Biosciences	Surface
CD3	AF700	SP34-2	BD Biosciences	Surface
CD8	APC-Cy7	RPA-T8	BD Biosciences	Surface
CD45	VD450	D058-1283	BD Biosciences	Surface

Supplemental Table 1. Fluorescently-labeled antibodies used in flow cytometry analysis.

	Monkey	Week	gB			gL		
			180.92	UCD52	UCD59	180.92	UCD52	UCD59
Viral Stocks	180.92	Stock	0.0037	0.0000	NA	0.0033	NA	NA
	UCD52	Stock	NA	0.0014	NA	NA	0.0025	NA
	UCD59	Stock	NA	0.0000	0.0030	NA	NA	0.0010
Control	145-97	1	NA	0.0003	0.0000	0.0073	0.0214	0.0230
	145-97	2	NA	0.0036	NA	0.0006	0.0052	NA
	145-97	6	0.0000	0.0075	0.0113	0.0013	0.0038	NA
	174-97	1	0.0018	0.0147	0.0050	NA	0.0095	0.0039
	174-97	3	0.0160	0.0091	0.0074	0.0028	0.0070	0.0077
	369-09	1	0.0066	0.0069	0.0082	0.0013	0.0046	0.0033
	369-09	2	NA	0.0122	0.0015	NA	0.0086	0.0049
	369-09	3	0.0059	0.0099	0.0156	0.0025	0.0052	0.0049
	369-09	5	NA	0.0089	0.0028	0.0000	0.0067	0.0054
	369-09	7	NA	0.0170	0.0148	0.0000	0.0037	NA
	369-09	9	NA	0.0029	0.0040	NA	0.0021	NA
	GM04	1	0.0000	0.0026	0.0124	0.0002	0.0049	0.0039
	GM04	2	0.0011	0.0148	0.0081	0.0013	0.0064	0.0015
	GM04	3	0.0088	0.0094	0.0067	0.0062	0.0035	0.0061
	GM04	4	0.0089	0.0046	0.0154	0.0036	0.0049	0.0029
	GM04	5	0.0034	0.0013	NA			
	HD79	1	0.0022	0.0012	0.0104	0.0048	0.0052	NA
	HD79	2	0.0041	0.0052	0.0011	0.0000	0.0004	NA
	HD79	3	0.0096	0.0009	0.0160	0.0000	0.0057	NA
	HD79	4	0.0028	0.0024	NA	0.0011	0.0043	NA
	HD79	5	0.0029	0.0027	NA	0.0033	0.0061	NA
	HD79	6	NA	0.0037	0.0032	0.0041	0.0000	NA
Standard HIG	GI73	1	NA	0.0149	0.0099			
	GI73	2	NA	0.0113	0.0015	0.0000	0.0114	0.0098
	GI73	3	NA	0.0130	0.0014	0.0058	0.0047	NA
	GI73	4	NA	0.0006	NA	0.0000	0.0196	0.0097
	GI73	5	0.0030	0.0080	0.0021	0.0024	0.0015	NA
	GI73	6	NA	0.0011	0.0119			
	IM67	1	0.0114	0.0060	0.0084	0.0003	0.0049	0.0023
	IM67	2	NA	0.0131	0.0027	0.0000	0.0060	NA
	IM67	3	0.0026	0.0026	0.0005	0.0000	0.0035	0.0062
	IM67	4	0.0050	0.0015	0.0010	0.0000	0.0005	NA
	IM67	5	0.0014	0.0139	0.0055	0.0000	0.0006	NA
	IM67	6	NA	0.0170	0.0112	0.0044	0.0138	0.0101
	JC65	1	NA	0.0062	0.0013	0.0000	0.0039	0.0008
	JC65	2	NA	0.0026	NA	NA	0.0053	0.0000
	JC65	3	NA	0.0035	0.0086	NA	0.0032	NA
	JC65	4	NA	0.0140	0.0027	0.0015	0.0000	NA
	JC65	5	NA	0.0008	0.0053	0.0005	0.0000	NA
	JC65	6	NA	0.0132	0.0014			
High-potency HIG	HD82	2	NA	0.0011	NA			
	HD82	3	NA	0.0053	0.0186	0.0039	0.0035	NA
	HD82	4	NA	0.0005	NA	0.0020	0.0028	NA
	HD82	6	0.0021	0.0000	NA	0.0056	0.0061	NA
	HR73	3	0.0018	NA	NA	0.0004	NA	NA
	HR73	4	NA	0.0007	0.0005	0.0003	0.0028	NA
	HR73	5	0.0023	0.0022	0.0000	0.0005	0.0010	NA
	HR73	6	0.0035	0.0037	0.0119	0.0044	0.0022	NA
	JM52	2	NA	0.0010	NA	0.0011	0.0020	NA
	JM52	3	0.0011	0.0020	0.0000			
	JM52	4	NA	0.0008	NA	NA	0.0032	NA
	JM52	5	NA	0.0006	NA	0.0011	NA	NA
	JM52	6	NA	0.0005	NA	0.0072	0.0055	NA

Supplemental Table 2. Raw nucleotide diversity values (π) for plasma variants at gB and gL loci

Group	Dam	Transmission Status (AF PCR)	Placental Tissue PCR	Placenta IHC	Microscopic findings
Control	369-09	+	+	+	No significant findings
	174-97	+	+	+	No significant findings
	274-98	+	+	-	No significant findings
	GM04	+	+	-	No significant findings
	HD79	+	+	+	No significant findings
Standard HIG	GI73	+	+	-	No significant findings
	IM67	+	+	+	Mild lymphocytic and neutrophilic infiltration.
	JC65	-	-	-	No significant findings
High-potency HIG	JM52	-	-	-	Minimal lymphocytic infiltration.
	HR73	-	-	-	No significant findings
	HD82	-	-	-	No significant findings

Supplemental Table 3. Immunohistochemical and microscopic findings in the placenta.

Gene ID	log2(fc)	P-value	Gene Title	Gene Description
CCL23	6.25	0.022	Chemokine (C-C Motif) Ligand 23	Small secreted protein chemotactic for resting T-cells and monocytes
SERPINA3	5.71	0.005	Serpin Peptidase Inhibitor, Clade A, Member 3	Plasma protease inhibitor upregulated during trauma and infection
KLK2	5.49	0.011	Kallikrein Related Peptidase 2	Grandular trypsin-like serine protease that cleaves at arginine residues
GNLY	5.21	0.008	Granulysin	Protein found in the granules of cytotoxic T cells and NK cells; induces apoptosis in target cells
OMD	5.06	0.009	Osteomodulin	Member of the small leucine-rich repeat proteoglycan family; involved in ECM during bone formation
POSTN	5.01	0.007	Periostin, Osteoblast Specific Factor	Secreted extracellular matric protein; binds to to integrin from epithelial cell adhesion and migration
GZMA	4.76	0.012	Granzyme A	Serine protease specific to cytotoxic T cells and NK cells; involved in lysing target cells
MAMU-A3	4.69	0.030	Major Histocompatibility Complex, Class I, A	Antigen-presenting molecules on cell surfaces
C13H2orf40	4.65	0.014	Chromosome 2 ORF 40	
RORB	4.63	0.027	RAR-Related Orphan Receptor B	Nuclear hormone receptor that binds to hormone response elements to regulate downstream genes
NDP	4.59	0.004	Norrie Disease (Pseudoglioma)	Secreted growth factor that activates the Wnt/beta-catenin pathway; mutations Norrie disease
ALDH1A2	4.19	0.019	Aldehyde Dehydrogenase 1 Family, Member A2	Enzyme that catalyzes the synthesis of retinoic acid from retinaldehyde
CRISP3	4.17	>0.001	Cysteine-Rich Secretory Protein 3	
CCL15	4.11	0.004	Chemokine (C-C Motif) Ligand 15	Small secreted protein chemotactic for neutrophils, T-cells, and monocytes
KLRB1	4.10	0.009	Killer Cell Lectin-Like Receptor B1	Membrane glycoprotein expressed by NK cells; involved in regulation of NK cells
GZMB	3.97	0.018	Granzyme B	Serine protease commonly found in the granules of CTLs, NK cells, and cytotoxic T cells
WT1	3.91	0.027	Wilms Tumor 1	Zinc finger transcription factor critical to the normal development of the urogenital system
CTSH	3.73	0.003	Cathepsin H	Cysteine protease critical to the degradation of lysosomal proteins
IGFBP6	3.67	0.018	Insulin-Like Growth Factor Binding Protein 6	Protein that regulates insulin-like growth factors
PRL	3.63	0.019	Prolactin	Anterior pituitary hormone acts as a growth regulator in many tissues; thought to suppress apoptosis
DKK1	3.57	0.006	Dickkopf WNT Signaling Pathway Inhibitor 1	Secreted protein that inhibits the WNT signaling pathway; critical to embryonic development
LYZ	3.54	0.001	Lysozyme	Antimicrobial enzyme that cleaves the bacterial cell wall peptidoglycan
IGFBP1	3.47	0.049	Insulin-Like Growth Factor Binding Protein 1	Protein that regulates insulin-like growth factors
APOD	3.38	0.002	Apolipoprotein D	Glycoprotein closely associated with the enzyme lectin cholestrol acyltransferase
FAP	3.29	0.011	Fibroblast Activation Protein, Alpha	Integral membrane gelatinase involved in fibroblast growth during development
CACNAD3	3.23	0.031	Voltage-Dependent Calcium Channel a2/d3	Member of a calcium channel complex that regulates calcium ion influx into the cell

Supplemental Table 4. Top 25 placental genes up-regulated in RhCMV infection

Gene ID	Log2(fc)	P-value	Gene Title	Function	Database
CCL2	1.29	0.002	C-C motif chemokine ligand 2	Chemoattractant for NK cells	IPA
CD44	1.06	0.027	CD44 molecule	Cytotoxic triggering molecule on activated NK cells	IPA
CD81	1.96	0.044	CD81 molecule	NK cell adhesion and trafficking	IPA
CXCL8	2.91	0.028	C-X-C motif chemokine ligand 8	Chemotaxis of NK cells	IPA
FYN	1.98	0.022	FYN protein tyrosine kinase	NK cell effector function	IPA
GZMB	3.97	0.018	granzyme B	Serine protease cytotoxic effector molecules	IPA
HLA-E	1.49	0.037	major histocompatibility complex, class I, E	Nonclassical antigen presentation to NK cells	KEGG
HLA-G	1.75	0.02	major histocompatibility complex, class I, G	Nonclassical antigen presentation to NK cells	IPA
IL1RL1	2.23	0.012	Interleukin 1 Receptor Like 1	Differentiation of NK cells	IPA
IL15	1.52	0.042	interleukin 15	Survival of peripheral NK cells	IPA
KIR2DL4	2.24	0.014	killer cell immunoglobulin like receptor	Activates NK cell cytotoxicity, recognizes HLA-G presentation	KEGG
KLRB1	4.1	0.009	killer cell lectin like receptor B1	Inhibits NK cell cytotoxicity	IPA
KLRC1 (CD94)	1.21	0.0002	killer cell lectin like receptor C1	Activates NK cell cytotoxicity, complexes with KLRD1 for HLA-E recognition	KEGG
KLRC3	1.78	0.005	killer cell lectin like receptor C3	Activates NK cell cytotoxicity	KEGG
KLRD1	1.75	0.015	killer cell lectin like receptor D1	Activates NK cell cytotoxicity, complexes with KLRC1 for HLA-E recognition	KEGG
NKG7	2.36	0.027	natural killer cell granule protein 7	Protein of unknown function on T and NK cells	KEGG
PRL	3.63	0.019	prolactin	NK cell activation, up-regulation of IL-2R	IPA
RARRES2	1.57	0.034	retinoic acid receptor responder 2	Chemoattractant for NK cells	IPA
SOCS2	1.26	0.01	suppressor of cytokine signaling 2	Regulates NK cell effector function in response to IL-15	IPA
TYROBP	1.13	0.049	TYRO protein tyrosine kinase binding protein	Activation of NK cells, complexes with KLRC1 (CD94)	IPA
VCAM1	2.91	0.031	vascular cell adhesion molecule 1	NK cell adhesion to endothelium	IPA

Supplemental Table 5. Placental genes up-regulated in RhCMV infection related to NK cell function and/or movement.